Design and performance analysis of a fan-shaped fractal antenna for radar systems and satellite communications

ABDELBASSET AZZOUZ[1], RACHID BOUHMIDI[1], MOHAMMED CHETIOUI[1], REDOUANE BERBER[1], AHMED JAMAL ABDULLAH AL-GBURI[2,*]
[1]*Laboratory of Electronics, Advanced Signal Processing, and Microwave (LESM), Department of Telecommunications, Saida University, Saida 20000, Algeria*
[2]*Strategic Research Institute (SRI), Asia Pacific University, Jalan Teknologi 5, Taman Teknologi Malaysia, 57000 Kuala Lumpur, Malaysia*

This study investigates the design and performance of a compact fan-shaped antenna optimized for radar and satellite communication applications. The proposed antenna, measuring 40 × 50 × 0.8 mm³, is fabricated on an FR4 substrate and fed using a 50 Ω microstrip line. Its performance was evaluated through full-wave simulations and validated experimentally using a Vector Network Analyzer. The antenna operates effectively at multiple resonant frequencies 2.05, 3.39, 5.34, 6.37, 7.38, 8.54, and 9.85 GHz achieving return loss values between −12.91 and −24.07 dB, with corresponding VSWR values from 1.13 to 1.58. A maximum gain of 9.11 dBi and bandwidths of up to 300 MHz were observed, with close agreement between simulated and measured results.

(Received August 14, 2025; accepted February 4, 2026)

Keywords: Fan-shaped antenna, Fractal antenna, Radar systems, Satellite communications

1. Introduction

In recent years, antenna design has witnessed significant advancements, particularly in the development of multiband, compact, and high-performance antennas for emerging applications such as RFID, IoT, 5G, and MIMO systems. Researchers have explored innovative antenna structures to meet the growing demand for efficient and versatile communication systems. Junho and Lee [1] proposed a small-form-factor wideband tapered slot antenna incorporating fan-shaped and stepped configurations for chipless RFID sensor-based tags. Similarly, Xue-Ping Li et al. [2] presented a low-profile bi-band microstrip antenna featuring fan-shaped and box-shaped elements, addressing the need for compact dual-band designs.

Further pushing the boundaries, Geeta Kalkhambkar et al. [3] introduced a wideband fractal antenna inspired by a snail-shell geometry, tailored for IoT applications, while Anuja Odhekar and Amit A. Deshmukh [4] designed a coplanar waveguide-fed microstrip antenna with a modified helicopter-fan shape, achieving circular polarization. Asma Khabba et al. [5] developed a compact O-shaped monopole MIMO antenna with self-decoupling capabilities for ultra-wideband (UWB) applications, offering excellent diversity and scalability for millimeter-wave 5G systems. In the UWB domain, P. More et al. [6] implemented a circular fan-shaped monopole patch radiator, and Atul Varshney et al. [7] presented a cost-effective ELC-configured UWB flared antenna with a parasitic SRR triad optimized for ISM and PCS frequency ranges. Additionally, Nirdosh et al. [8] enhanced a four-element fan-profile MIMO antenna with improved bandwidth for high-capacity communication. Advances in optimization techniques have further contributed to antenna development. Hsi-Tseng Chou et al. [9] optimized multi-beam radiation from a two-dimensional dielectric lens antenna using genetic algorithms to enhance beam overlap. Masahiro and Nakano [10] developed a compact wideband planar spiral radiator featuring a circular high-impedance surface reflector composed of identical fan-contoured patches. In the context of waveguide technology, Han et al. [11] proposed a small-form half-mode fan-shaped substrate integrated waveguide frequency-selective network with adjustable order and broad stopband. Sergey Churkin et al. [12] introduced arrays of microstrip patch fan-contoured antennas with radiation patterns optimized for MIMO at 28 GHz, while Andrey Mozharovskiy et al. [13] designed 28 GHz waveguide-based radiators featuring fan-contoured coverage patterns for base stations. Lastly, V. N. Koteswara and Rao [14] optimized a flared fan-type UWB antenna with a band-reject design for WLAN integration using a basic non-driven slot.

This body of work highlights the versatility and potential of fan-shaped and fractal antenna designs for modern communication systems. Building on these advancements, the proposed antenna operates at multiple resonant frequencies spanning 2.05 to 9.85 GHz, corresponding to several important practical applications. Lower resonances near 2.05 GHz are suitable for S-band radar and satellite telemetry, while mid-band frequencies around 3.39 and 5.34 GHz align with C-band radar, satellite downlinks, and wireless communication services. Higher resonances between 6.37 and 9.85 GHz cover portions of the X-band, supporting applications such as high-resolution radar, Earth-observation satellites, and deep-space communication links. By targeting these key frequency ranges, the proposed fan-contoured fractal radiator is optimized for a broad set of radar and space-

based communication systems, with detailed performance evaluations presented in the following sections.

The paper proceeds as follows: Section 2 outlines the design methodology of the proposed fan-shaped fractal antenna, detailing the materials, dimensions, iterative antenna geometry, and the integration of the microstrip feed line. Section 3 presents and analyzes simulation outcomes and measurement results, focusing on resonant frequencies, return loss, bandwidth, VSWR, and gain, as well as the impact of feed width and dielectric material on performance. Finally, Section 4 summarizes the key results of the study.

2. Antenna design

Fig. 1 shows a top view of the proposed fan-shaped fractal antenna, with overall dimensions of 40 × 50 × 0.8 mm³. The antenna is fabricated on an FR4 substrate with a relative permittivity (εr) of 4.7, a loss tangent (tan δ) of 0.0197, and a 35 µm copper layer, featuring a full ground plane. It is energized using a 50 Ω microstrip feed line to ensure efficient impedance matching and signal transmission.

The antenna design follows a fractal iteration process, as illustrated in Fig. 2. The design begins with a zero iteration, which consists of a large central circle connected to the feed line, along with symmetrically arranged rectangular shapes. In the first iteration, a smaller circle is added inside the central circle, and the rectangular shapes are rotated by −90° relative to the feed line, improving multiband performance. The second iteration introduces an even smaller circle and rectangular shapes rotated by 180°, further optimizing impedance matching and gain. In the final iteration, another smaller circle is added, along with rectangular shapes rotated by +90° relative to the feed line, maximizing the antenna's bandwidth and gain. The antenna's performance was evaluated through full-wave simulations using HFSS, and Table 1 lists all key design parameters.

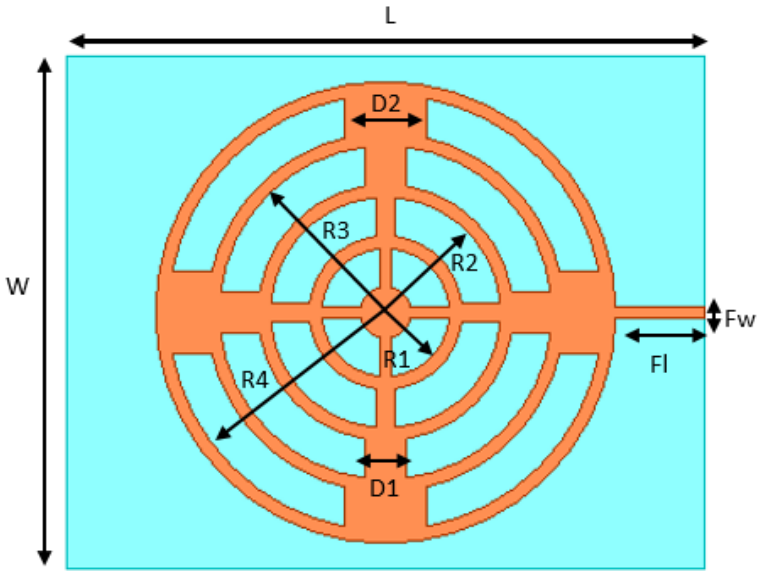

Fig. 1. Top view of the proposed antenna (colour online)

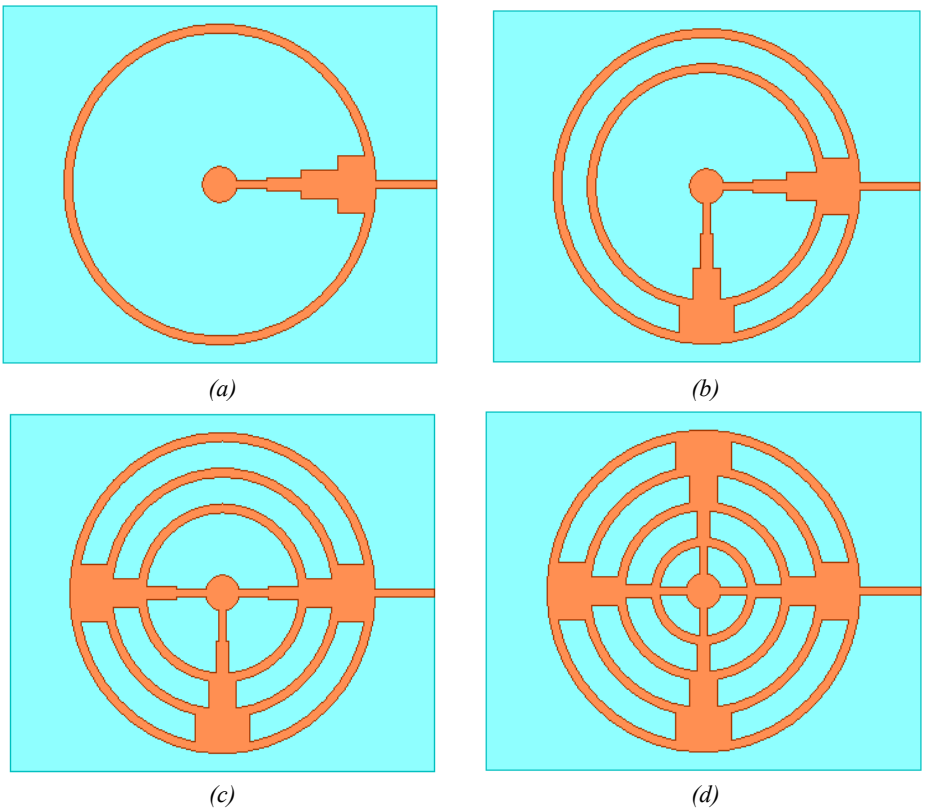

Fig. 2. Iteration stages of the proposed antenna (colour online)

Table 1. Parameters of the proposed antenna and their values

Variables	Values(mm)	Variables	Values(mm)
W	40	L	50
R1	5	R2	9
R3	13	R4	17
Fw	1.45	Fl	7
D1	3.20	D2	6.40

3. Results and discussion

3.1. Return Loss and VSWR

The return loss performance of the proposed fan-shaped fractal antenna was evaluated across multiple resonant frequencies. The antenna operates efficiently over several frequency bands, with resonances occurring at 2.05, 3.39, 5.34, 6.37, 7.38, 8.54, and 9.85 GHz. The corresponding return loss values are −12.91, −17.08, −18.48, −16.52, −15.19, −14.74, and −24.07 dB, indicating strong impedance matching across the spectrum. The lowest return loss of −24.07 dB is observed at 9.85 GHz, signifying excellent reflection coefficient performance at this frequency.

The antenna exhibits a Voltage Standing Wave Ratio (VSWR) of 1.58, 1.35, 1.27, 1.35, 1.42, 1.45, and 1.13 at the respective resonant frequencies, all well below the acceptable limit of 2.0, further confirming good impedance matching and efficient power transfer. The optimal VSWR of 1.13 occurs at 9.85 GHz, consistent with the lowest return loss at this frequency. Additionally, the antenna achieves a maximum bandwidth of 300 MHz, ensuring stable performance over a wide frequency range. These return loss and VSWR results demonstrate the antenna's suitability for radar and satellite communication applications, providing minimal signal reflection and efficient radiation across multiple bands.

Fig. 3 illustrates the effects of varying the feed width on antenna performance, highlighting how feed adjustments influence return loss and bandwidth. Fig. 4 examines the impact of different dielectric materials on antenna characteristics, showing that the FR4 substrate delivers the most stable performance. Fig. 5 presents the return loss characteristics for each design iteration, where progressive improvements are observed as smaller circles and rectangular shapes are added. Finally, Fig. 6 compares the simulated and measured return loss values, demonstrating close agreement and validating the accuracy of the simulations.

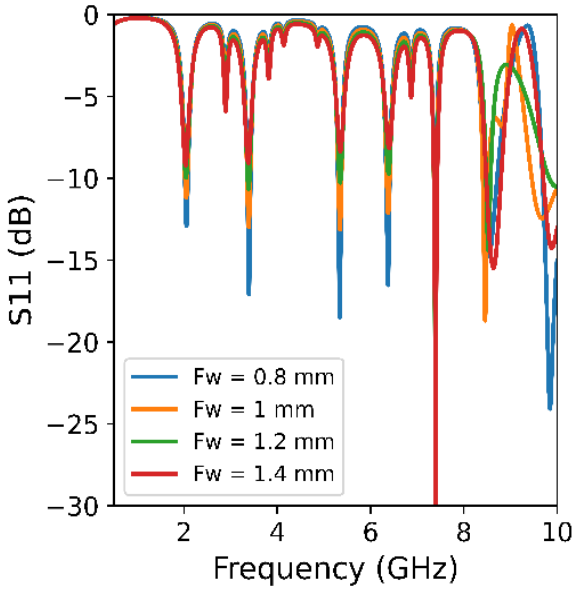

Fig. 3. Effect of feed width variation on the proposed antenna (colour online)

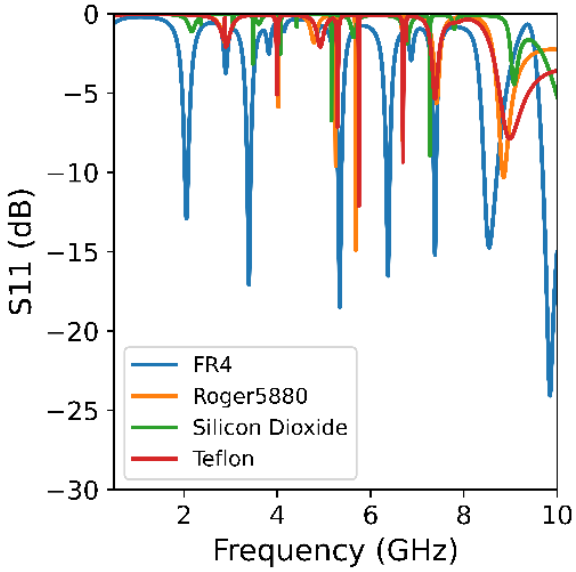

Fig. 4. Effect of dielectric materials on the proposed antenna (colour online)

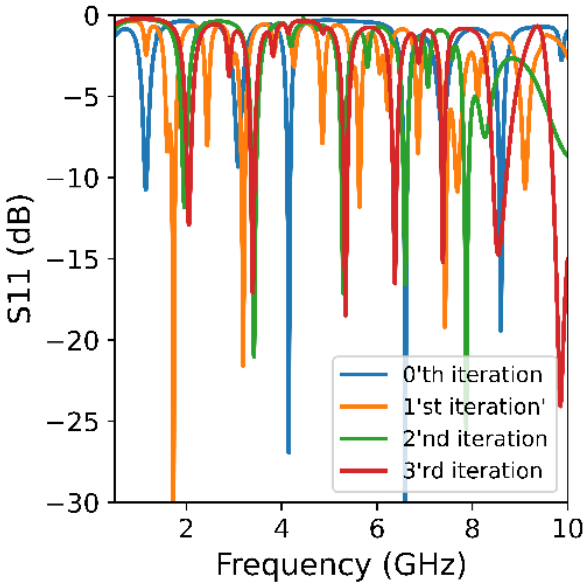

Fig. 5. Return loss versus frequency for each iteration (colour online)

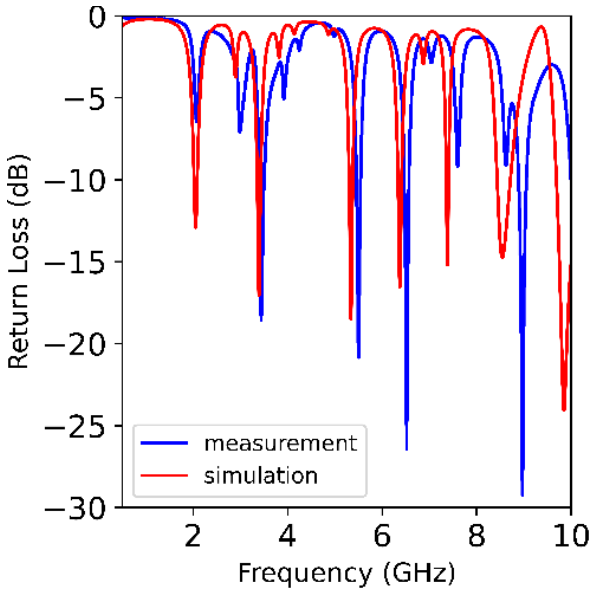

Fig. 6. Simulated and measured return loss of the antenna (colour online)

3.2. Radiation pattern and gain

The radiation pattern and gain of the proposed fan-shaped fractal antenna were thoroughly evaluated to assess its effectiveness for radar and satellite communication systems. The antenna achieves a maximum gain of 9.11 dBi, indicating strong directional capability and efficient signal transmission.

Fig. 7 presents the radiation patterns at each resonant frequency for both the E-plane (φ = 0°) and H-plane (φ = 90°), where the blue line represents the E-plane and the red line represents the H-plane. The radiation patterns reveal that the antenna provides broad omnidirectional coverage in the H-plane while exhibiting more focused radiation in the E-plane. This behavior demonstrates the antenna's ability to efficiently radiate energy over a wide angular range in one plane while concentrating the energy in a specific direction in the other plane, which is advantageous for targeted communication applications.

Fig. 8 illustrates the gain characteristics at each resonant frequency. The gain values are consistent with the observed radiation patterns, showing that the antenna maintains high efficiency and strong performance across its operational bandwidth. The peak gain of 9.11 dBi is achieved at the higher resonant frequencies, highlighting the antenna's capability to deliver robust signal strength and reliable performance.

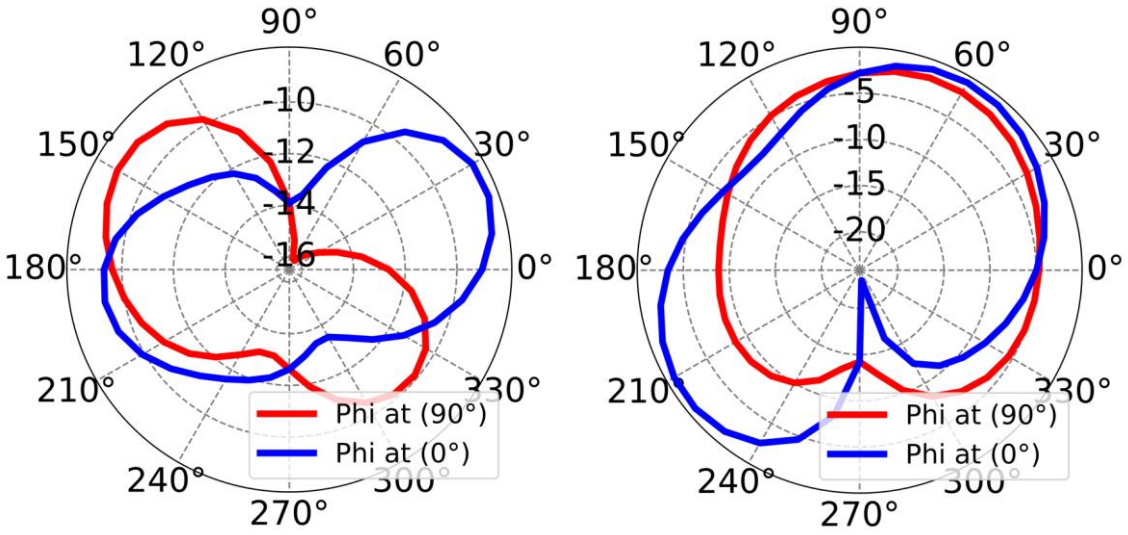

(a) *(b)*

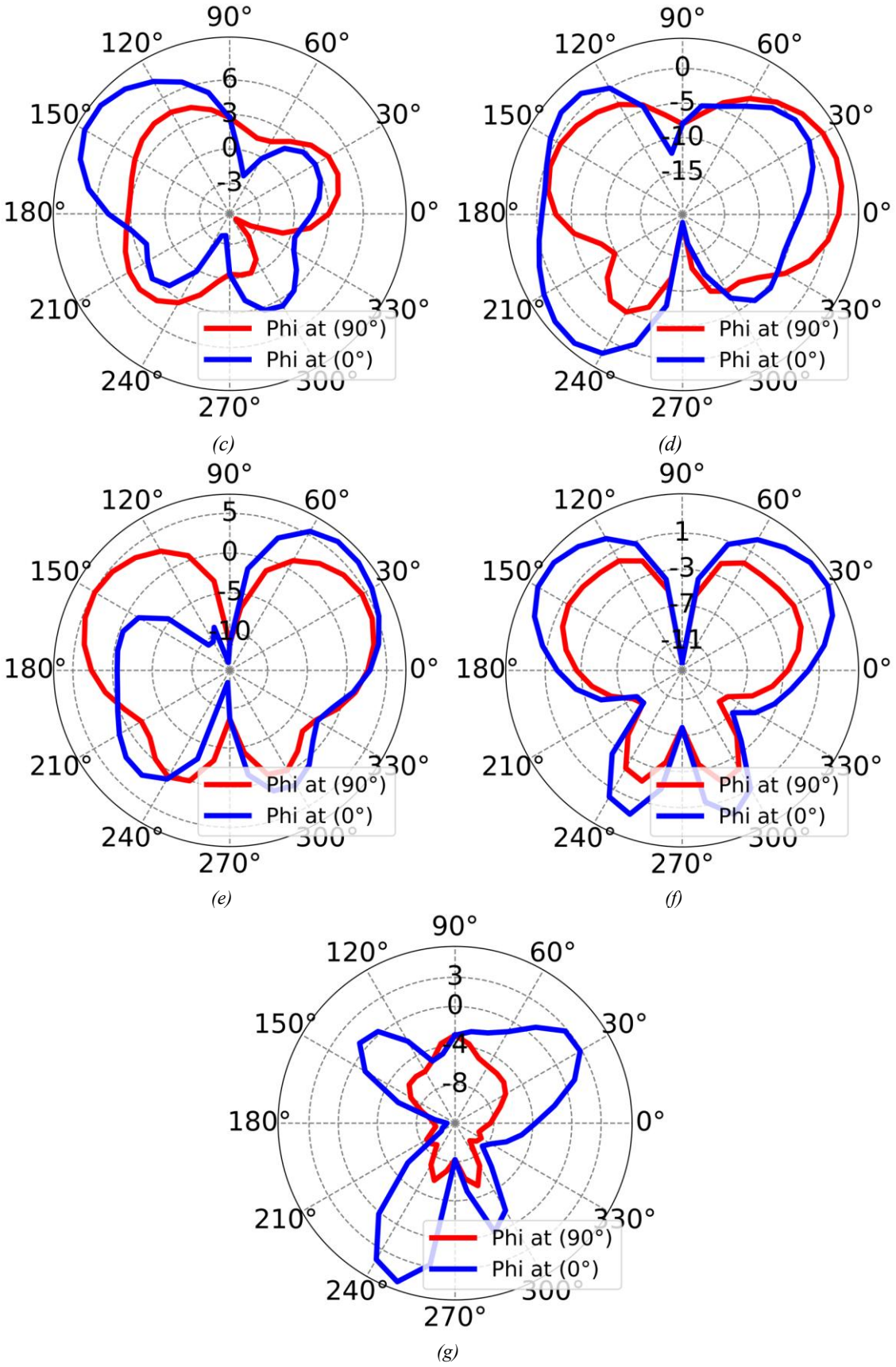

Fig. 7. Radiation pattern characteristics of the proposed antenna at (a) 2.05 GHz, (b) 3.39 GHz, (c) 5.34 GHz, (d) 6.37 GHz, (e) 7.38 GHz, (f) 8.54 GHz, and (g) 9.85 GHz (colour online)

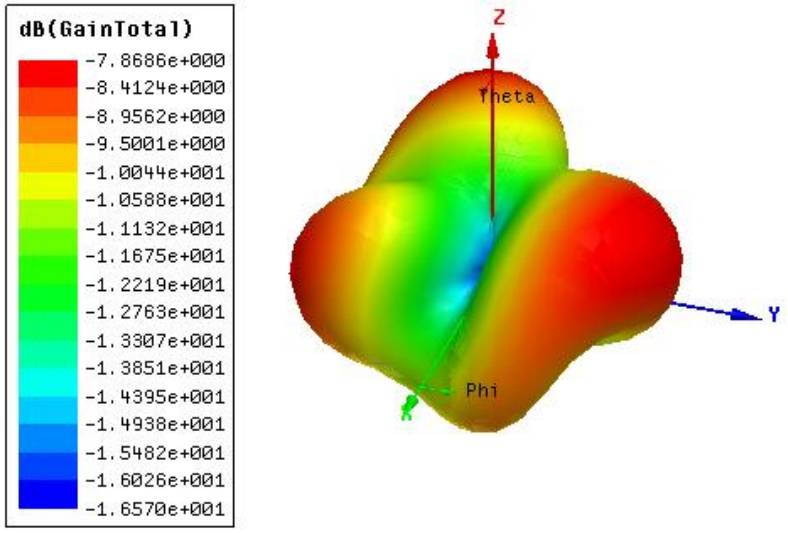
dB(GainTotal)
-7.8686e+000
-8.4124e+000
-8.9562e+000
-9.5001e+000
-1.0044e+001
-1.0588e+001
-1.1132e+001
-1.1675e+001
-1.2219e+001
-1.2763e+001
-1.3307e+001
-1.3851e+001
-1.4395e+001
-1.4938e+001
-1.5482e+001
-1.6026e+001
-1.6570e+001
Z
Theta
Y
Phi

(a)

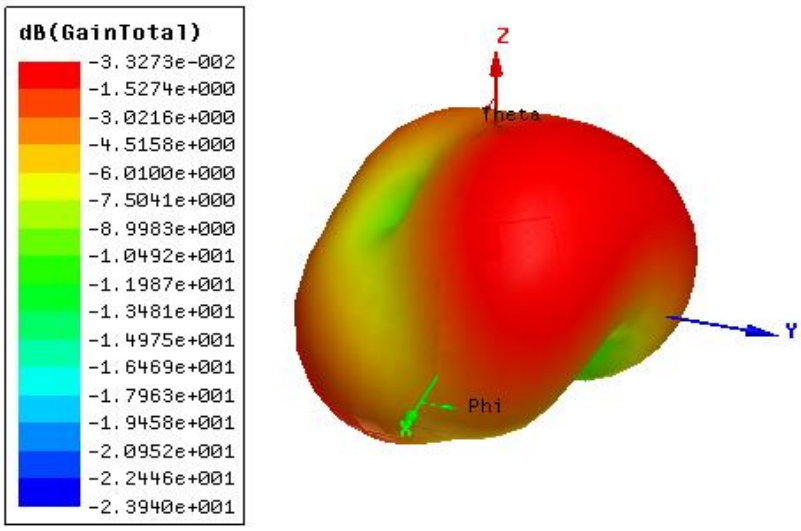
dB(GainTotal)
-3.3273e-002
-1.5274e+000
-3.0216e+000
-4.5158e+000
-6.0100e+000
-7.5041e+000
-8.9983e+000
-1.0492e+001
-1.1987e+001
-1.3481e+001
-1.4975e+001
-1.6469e+001
-1.7963e+001
-1.9458e+001
-2.0952e+001
-2.2446e+001
-2.3940e+001
Z
Theta
Y
Phi

(b)

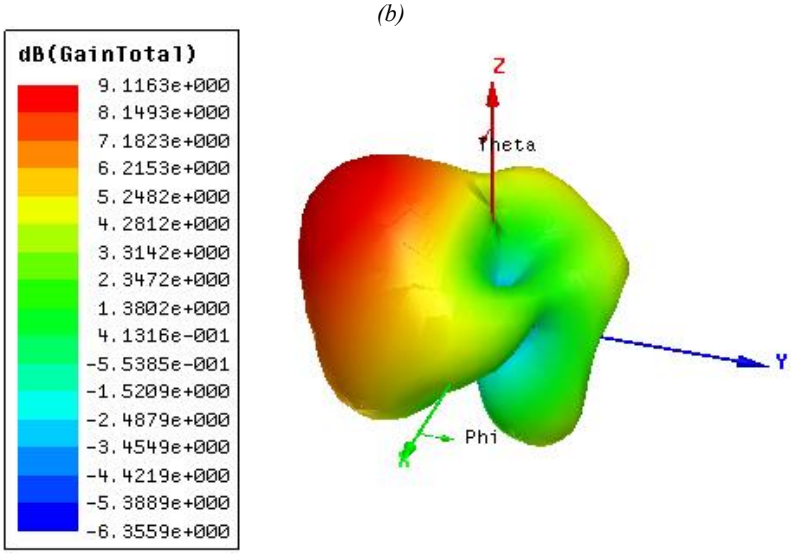
dB(GainTotal)
9.1163e+000
8.1493e+000
7.1823e+000
6.2153e+000
5.2482e+000
4.2812e+000
3.3142e+000
2.3472e+000
1.3802e+000
4.1316e-001
-5.5385e-001
-1.5209e+000
-2.4879e+000
-3.4549e+000
-4.4219e+000
-5.3889e+000
-6.3559e+000
Z
Theta
Y
Phi

(c)

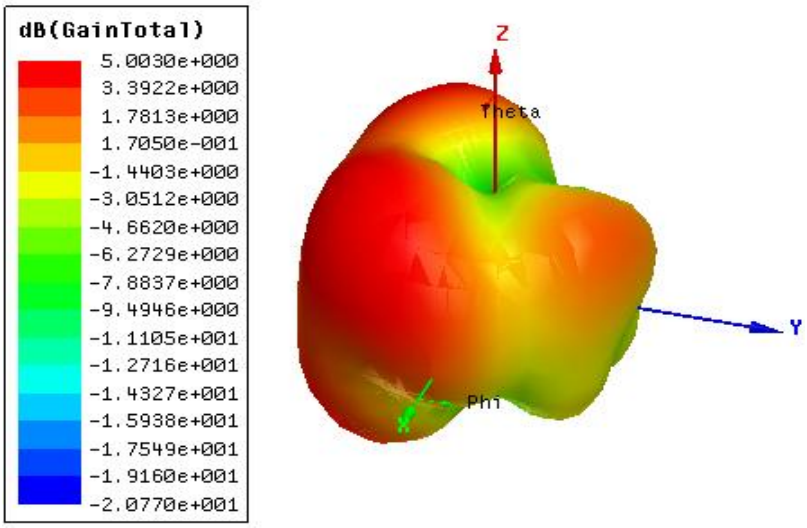
dB(GainTotal)
5.0030e+000
3.3922e+000
1.7813e+000
1.7050e-001
-1.4403e+000
-3.0512e+000
-4.6620e+000
-6.2729e+000
-7.8837e+000
-9.4946e+000
-1.1105e+001
-1.2716e+001
-1.4327e+001
-1.5938e+001
-1.7549e+001
-1.9160e+001
-2.0770e+001
Z
Theta
Y
Phi

(d)

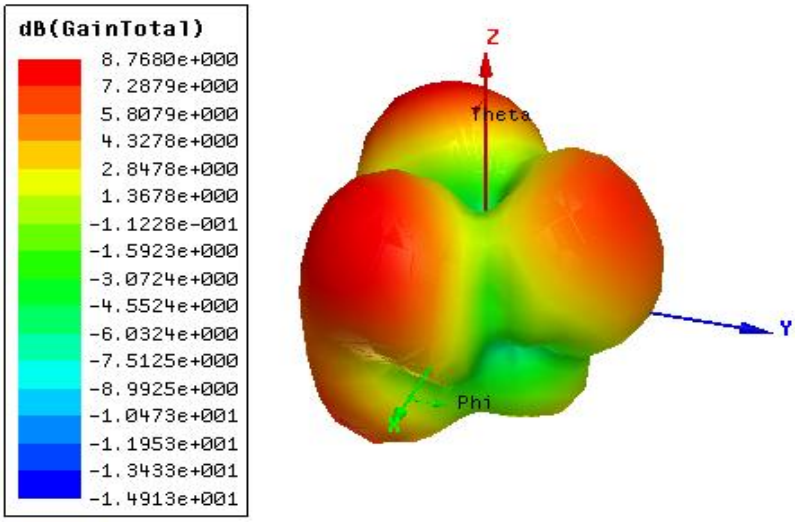
dB(GainTotal)
8.7680e+000
7.2879e+000
5.8079e+000
4.3278e+000
2.8478e+000
1.3678e+000
-1.1228e-001
-1.5923e+000
-3.0724e+000
-4.5524e+000
-6.0324e+000
-7.5125e+000
-8.9925e+000
-1.0473e+001
-1.1953e+001
-1.3433e+001
-1.4913e+001
Z
Theta
Y
Phi

(e)

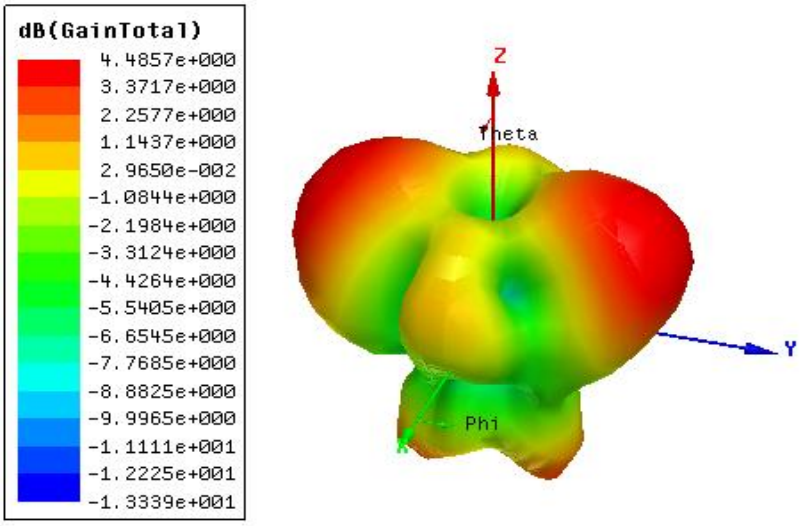
dB(GainTotal)
4.4857e+000
3.3717e+000
2.2577e+000
1.1437e+000
2.9650e-002
-1.0844e+000
-2.1984e+000
-3.3124e+000
-4.4264e+000
-5.5405e+000
-6.6545e+000
-7.7685e+000
-8.8825e+000
-9.9965e+000
-1.1111e+001
-1.2225e+001
-1.3339e+001
Z
Theta
Y
Phi

(f)

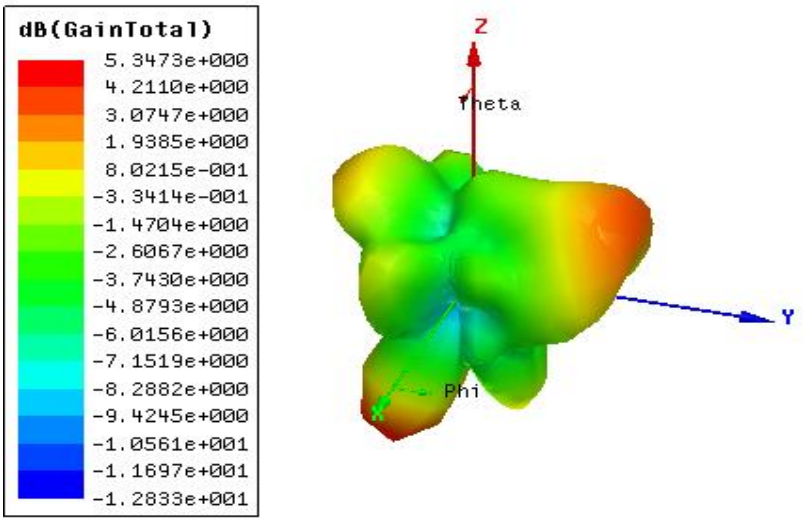

(g)

Fig. 8. Gain characteristics of the proposed antenna at (a) 2.05 GHz, (b) 3.39 GHz, (c) 5.34 GHz, (d) 6.37 GHz, (e) 7.38 GHz, (f) 8.54 GHz, and (g) 9.85 GHz (colour online)

3.3. Current distribution

Surface current distribution patterns were analyzed to understand how electrical currents are distributed across the antenna structure at various resonant frequencies. Fig. 9 shows the current distribution at key resonant frequencies, including 2.05, 3.39, 5.34, 6.37, 7.38, 8.54, and 9.85 GHz. The current distributions exhibit distinct patterns corresponding to the antenna's geometric features and resonant modes.

At lower frequencies, such as 2.05 and 3.39 GHz, the current is primarily concentrated along the edges of the fractal shapes and the feed line. This edge concentration enhances the antenna's ability to efficiently radiate and receive signals at these frequencies. At higher resonant frequencies, particularly 8.54 and 9.85 GHz, the current shifts toward the smaller fractal elements and central regions of the antenna. This shift demonstrates that the antenna design effectively utilizes the fractal geometry to improve performance at higher frequencies.

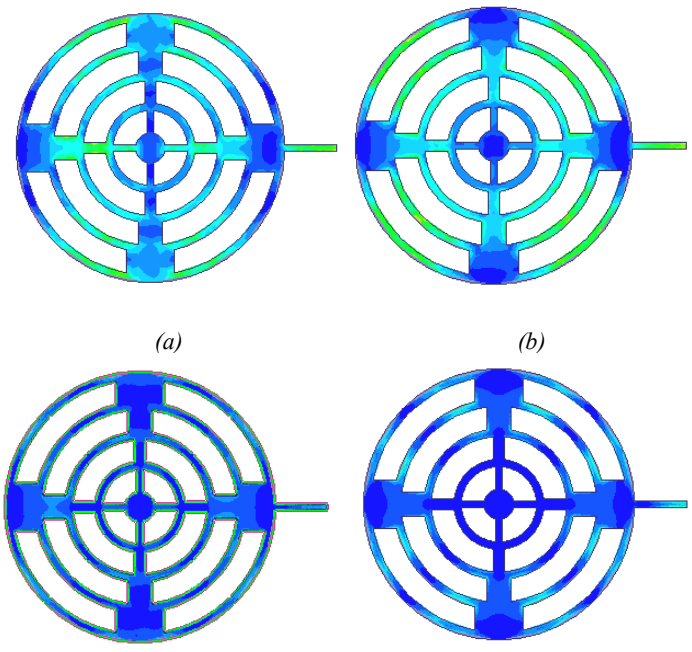

(a) *(b)*

(c) *(d)*

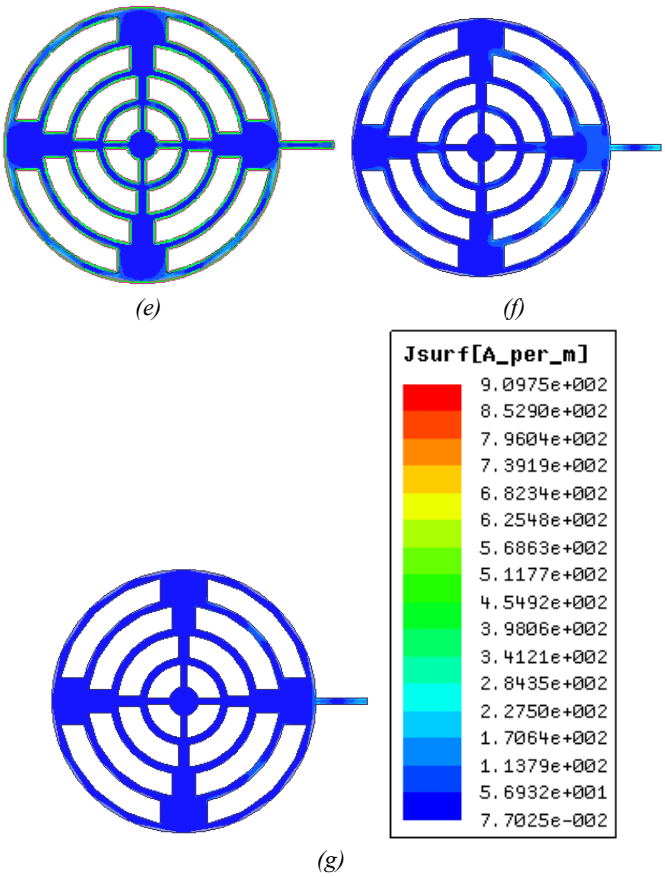

Fig. 9. Surface current distribution characteristics of the proposed antenna at (a) 2.05 GHz, (b) 3.39 GHz, (c) 5.34 GHz, (d) 6.37 GHz, (e) 7.38 GHz, (f) 8.54 GHz, and (g) 9.85 GHz (colour online)

The fabricated proposed antenna is shown in Fig. 10. A comparison of antenna designs in Table 2 highlights key differences in terms of size, operating bands, dielectric materials, and maximum gain, providing insight into the capabilities of the proposed fan-shaped fractal radiator relative to existing designs. The proposed antenna (Prop, 2024) is distinguished by its compact size of 40 × 50 mm², significantly smaller than the compared designs, while operating across seven frequency bands. This represents a substantial improvement in multiband performance, as most other antennas typically support only two or three bands. For example, the design by [2] (2023) covers only two bands with a larger size of 70 × 90 mm², while [17] (2021) supports three bands at a much larger dimension of 87 × 100 mm².

Regarding dielectric materials, the proposed antenna uses FR4 with a relative permittivity (εr) of 4.7 and a loss tangent (tan δ) of 0.0197. Although FR4 is generally considered less suitable for high-performance RF applications due to its higher loss tangent, the antenna achieves an impressive maximum gain of 9.11 dBi. This surpasses other designs, such as the antenna by [2], which achieves 8.2 dBi using F4BM220, a substrate with superior RF characteristics. Additionally, designs employing RO4350 and RO4350B substrates, such as those by [15] and [16], report gains of 4.4 dBi and 7.35 dBi, respectively. Although these materials have lower loss, they do not achieve the gain performance demonstrated by the proposed design.

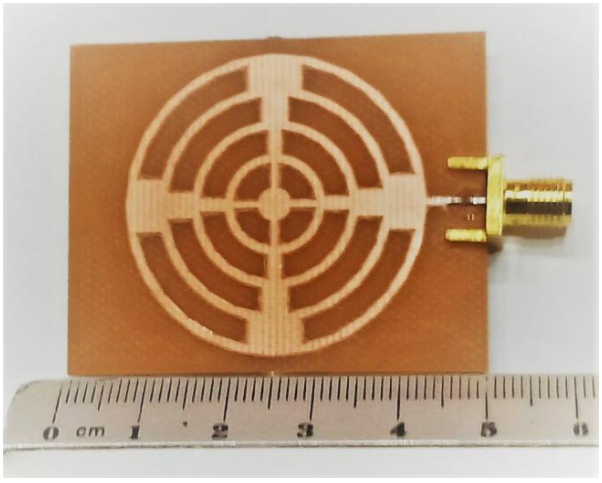

Fig. 10. Fabricated proposed fan-shaped antenna (colour online)

The antenna presented in [17] exhibits a significantly low gain of −38.5 dBi, which may be attributed to its larger size and the use of RT/duroid 5880. Although this substrate has excellent dielectric properties, it appears to have been implemented in an inefficient design. In contrast, the proposed antenna achieves an optimal balance between compact size, multiband operation, and high gain,

demonstrating the effectiveness of its design compared to more conventional approaches. This makes it well-suited for modern applications that require both small form factors and high performance across multiple frequency bands.

Table 2. Design parameters and associated values for the proposed antenna

Ref	Year	Size (mm^2)	No. bands	Dielect-material	gain (dBi)
Prop	2024	40×50	7	FR4	9.11
[2]	2023	70×90	2	F4B	8.2
[15]	2023	52×71	2	RO4	4.4
[16]	2023	65×65	2	RO4	7.35
[17]	2021	87×100	3	duroid	-38.5

3. Conclusion

The fan-shaped fractal antenna designed for radar and satellite communication systems demonstrates robust performance across a wide frequency spectrum. Its effective operation at resonant frequencies ranging from 2.05 to 9.85 GHz, combined with substantial return loss values and an impressive bandwidth of up to 300 MHz, underscores strong impedance matching and broad frequency response. The low VSWR values further confirm the antenna's efficiency in signal transmission. With a maximum gain of 9.11 dBi, the antenna achieves high performance, and the close agreement between simulated and measured results validates the design's effectiveness. This antenna represents a significant advancement in high-frequency antenna technology, providing reliable and efficient performance for radar and satellite communication applications.

Acknowledgements

The authors express their sincere gratitude to Asia Pacific University (APU) and the Strategic Research Institute (SRI) for supporting this project.

References

[1] J. Yeo, J.-I. Lee, Sensors **24**(12), 3835 (2024).
[2] X.-P. Li, M.-M. Li, J.-F. Ji, Q.-Q. Sun, W. Li, A.-X. Zhang, Electronics **12**(19), 4040 (2023).
[3] G. Kalkhambkar, R. Khanai, P. Chindhi, Arabian Journal for Science and Engineering **48**(11), 15463 (2023).
[4] A. Odhekar, A. A. Deshmukh, Proceedings of International Conference on Wireless Communication: ICWiCom 2021, Springer, 39 (2022).
[5] A. Khabba, J. Amadid, S. Mohapatra, Z. El Ouadi, S. Ahmad, S. Ibnyaich, A. Zeroual, Applied Physics A **128**(8), 725 (2022).
[6] P. More, A. Patil, G. Patil, K. Thakur, D. Marathe, International Journal of Wireless and Microwave Technologies **11**(2), 32 (2021).
[7] A. Varshney, N. Cholake, V. Sharma, International Journal of Electronics Letters **10**(4), 391 (2022).
[8] A. Kakkar, M. R. Tripathy, 7th International Conference on Signal Processing and Integrated Networks (SPIN), IEEE, 384 (2020).
[9] H.-T. Chou, Y.-S. Chang, H.-J. Huang, Z.-D. Yan, T. Lertwiriyaprapa, D. Torrungrueng, IEEE Access **8**, 79124 (2020).
[10] M. Tanabe, H. Nakano, IEEE Transactions on Antennas and Propagation **68**(10), 7219 (2020).
[11] H.-Y. Xie, B. Wu, L. Xia, J.-Z. Chen, T. Su, IEEE Microwave and Wireless Components Letters **30**(8), 749 (2020).
[12] S. Churkin, A. Mozharovskiy, A. Artemenko, R. Maslennikov, 12th European Conference on Antennas and Propagation (EuCAP 2018).
[13] A. Mozharovskiy, S. Churkin, A. Artemenko, R. Maslennikov, 12th European Conference on Antennas and Propagation (EuCAP 2018).
[14] V. K. R. Devana, A. M. Rao, International Journal of Electronics Letters **7**(3), 352 (2019).
[15] R. Kalaiyarasan, G. Nagarajan, S. Seenuvasamurthi, e-Prime-Advances in Electrical Engineering, Electronics and Energy **6**, 100320 (2023).
[16] M. Y. I. Yazid, M. H. Baharuddin, M. S. Islam, M. T. Islam, A. F. Almutairi, IEEE Access **11**, 32335 (2023).
[17] I. Masroor, S. Aslam, 2021 IEEE Texas Symposium on Wireless and Microwave Circuits and Systems (WMCS), IEEE, 1 (2021).

*Corresponding author: ahmedjamal@ieee.org
ahmedjamal@utem.edu.my